ELSEVIER

Biophysical Chemistry 125 (2007) 286–297

Biophysical Chemistry

http://www.elsevier.com/locate/biophyschem

The effects of time delays in a phosphorylation–dephosphorylation pathway

J. Srividhya [a,*], M.S. Gopinathan [b], Santiago Schnell [a]

[a] *Complex Systems Group, Indiana University School of Informatics and Biocomplexity Institute, 1900, East Tenth Street, Bloomington, IN 47406, USA*
[b] *Indian Institute of Information Technology and Management Kerala, Thiruvananthapuram, Kerala 695581, India*

Received 29 June 2006; received in revised form 31 August 2006; accepted 3 September 2006
Available online 2 October 2006

Abstract

Complex signaling cascades involve many interlocked positive and negative feedback loops which have inherent delays. Modeling these complex cascades often requires a large number of variables and parameters. Delay differential equation models have been helpful in describing inherent time lags and also in reducing the number of governing equations. However the consequences of model reduction via delay differential equations have not been fully explored. In this paper we systematically examine the effect of delays in a complex network of phosphorylation–dephosphorylation cycles (described by Gonze and Goldbeter, *J. Theor. Biol.*, 210, (2001) 167–186), which commonly occur in many biochemical pathways. By introducing delays in the positive and negative regulatory interactions, we show that a delay differential model can indeed reduce the number of cycles actually required to describe the phosphorylation–dephosphorylation pathway. In addition, we find some of the unique properties of the network and a quantitative measure of the minimum number of delay variables required to model the network. These results can be extended for modeling complex signalling cascades.

Keywords: Phosphorylation–dephosphorylation; Dominoes; Oscillations; Delay differential equations; Delayed regulation

1. Introduction

Cells use a complex network of interacting molecular components to transfer and process information. These biochemical pathways are responsible for many important cellular processes, including cell cycle regulation and signal transduction cascades. Reversible phosphorylation–dephosphorylation (PD) cycles form the skeleton of the networks containing these signalling metabolic cascades. Reversible PD helps in modulating the functional properties of proteins involved in gene expression [1], cell adhesion [2], cell cycle regulation [3], cell proliferation [4] and differentiation [5]. PD cycles are enzymatic processes which are in turn regulated, often in several steps, allowing amplification and fine control.

In cellular signalling networks, PD cycles are sometimes knit together like a cascade involving a series of activations, for example the phosphorylated product of one PD cycle activating the subsequent phosphorylation reaction and so on. These cycles may have comparable rates. The dynamics of the cell cycle can be described as a sequential PD [6] cascade similar to a domino effect. Modeling these cascades with ordinary differential equations (ODEs) involves a large number of variables and parameters, which makes the analysis of these models cumbersome. Modeling such systems with delay differential equations (DDEs) helps to describe the important dynamics with fewer variables and parameters.

Time lags are ubiquitous in biological systems. Delays manifest in the form of aging time, gene expression time, incubation time etc. These delays are observed in biological systems and hence mathematical models of these systems with DDEs have been highly successful. The glucose-insulin dynamical system has been successfully modeled with a state dependent delay [7]. The importance of inter-compartmental delay in human gastric acid secretion has been described with the use of DDEs [8]. A two-delay model for erythropoiesis [9,10] describes the effect of age-structured delay as seen in experimental observations. Feedback regulation in the lactose operon has been modeled by delay differential equations and has been shown to agree very well with the experimental data

* Corresponding author. Tel.: +1 812 856 2226; fax: +1 812 856 1995.
E-mail address: sjeyaram@indiana.edu (J. Srividhya).

0301-4622/$ - see front matter © 2006 Elsevier B.V. All rights reserved.
doi:10.1016/j.bpc.2006.09.001

[11]. Further, it has also been shown mathematically that oscillatory expression of proteins in cultured mammalian cells is most likely driven by transcriptional delays [12]. In all the above examples, the DDE models describe biologically relevant time lags. Alternately, DDEs can lead to very simple models that aid in conceptual understanding of the dynamics. Delays in circadian rhythms have been shown to describe the dynamics with fewer variables and parameters [13–15].

Delay has been used to model complex systems. However, few studies are available to describe the effect of delays in general biochemical systems [16,17]. The effect of distributed delays in simple enzyme kinetics has been shown to replace several intermediate complexes [18]. Similar studies on general aspects of biochemical pathways can provide useful information while undertaking modeling of complex systems.

Since PD cycle cascades occur frequently in biochemical pathways, the effect of delays in these cascades could reveal valuable information about modeling similar systems. The ODE model by Gonze and Goldbeter [19] describes a generic form of PD network that frequently occur in many biochemical pathways. The model provides an example of a biochemical network as described by Murray and Kirshner [6].

Therefore, the primary objective of this study is to examine whether delayed regulatory steps in a PD cascade can reduce the number of cycles actually required to describe the dynamics. To test this we modify the ODE model for the coupled PD network described in Ref. [19] by introducing delayed regulatory loops. In Section 2, we show that delay in a positive regulatory step can effectively replace alternate cycles in a network. We then discuss the bifurcation diagrams for the delay equations and compare the results with that of the ODE model. In Section 3, we show that, under symmetrical parameters condition, the stability properties of the delayed system can be determined analytically. We quantitatively predict how many cycles can be replaced with delayed variables, which can be used as a reference table when modeling complex biological systems. This is followed by a discussion (Section 4).

2. Reduced model with delayed positive regulation

We start by giving a brief account of the ODE model [19]. A network of four (N=4) PD cycles (I, II, III and IV) is coupled through positive and negative regulatory effects in a cyclic manner as described in Fig. 1. The solid lines denote positive regulation and dashed lines denote negative regulation. A given cycle experiences a positive regulation by $i-1$th cycle and a negative regulation by $i+2$th cycle.

In each cycle, a dephosphorylated protein Y_i is transformed into the phosphorylated form X_i by an enzyme E_i of maximum rate V_{Mi} and Michaelis–Menten constant K, while the reverse transformation is catalyzed by an enzyme E_i' with maximum rate V_{Mi}' and Michaelis–Menten constant K'. The cofactors in the reaction are considered as constant. The phosphorylation is activated (positive regulation) by X_{i-1} and the dephosphorylation is activated (negative regulation) by X_{i+2}. The corresponding Michaelis–Menten constants for the both the processes are K_{ai} and K_{bi}. α_i and β_i are the strengths of positive and negative regulations respectively. We can express this interaction mathematically for N cycles as follows

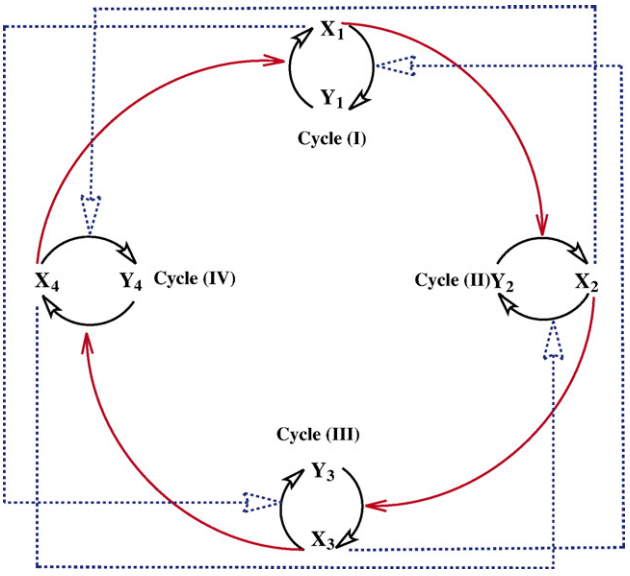

Fig. 1. Schematic representation of phosphorylation–dephosphorylation cycle network according to Gonze and Goldbeter [19] for N=4. X_i is the phosphorylated form and Y_i is the dephosphoryated form. A cycle experiences a positive regulation by $i-1$th cycle and a negative regulation by $i+2$th cycle. The red solid lines correspond to positive regulation and the blue dashed lines correspond to negative regulation. (For interpretation of the references to colour in this figure legend, the reader is referred to the web version of this article.)

$$\frac{dX_i}{dt} = V_{Mi}\left[1+\alpha_i\frac{X_{i-1}}{K_a+X_{i-1}}\right]\frac{(1-X_i)}{K+(1-X_i)} - V_{Mi}'\left[1+\beta_i\frac{X_{i+2}}{K_b+X_{i+2}}\right]\frac{X_i}{K'+X_i}(i=1,2,\ldots,N). \quad (1)$$

For N=4 there are four ODEs that describe the scheme in Fig. 1. The concentrations of the PD pairs are scaled to unity ($X_i+Y_i=1$). Hence, the dephosphorylated form Y_i is written as $Y_i=1-X_i$ in the above equation. Here, owing to the cyclic nature of the networks, i is modulo N such that $N+1$ is 1.

Now let us reduce the system. In the present case, instead of involving four variables, we replace the cycle II and cycle IV of the ODE model with a delayed positive interaction between cycle I and cycle III. In other words, the sequential activation between three species is considered as a delayed activation between two species. Fig. 2 shows the schematic diagram of the delayed positive regulation. In this case positive regulatory steps alone are delayed and negative regulation is maintained as instantaneous.

The governing equations are obtained by reducing the N=4, (X_1, X_2, X_3, X_4), ODE model with delay in the positive regulation. The parameters along with the equations are given in Table 1. The parameter set in Table 1 represent a symmetrical situation where all the maximum rates and regulation strengths are equal to unity and the Michaelis–Menten constants are

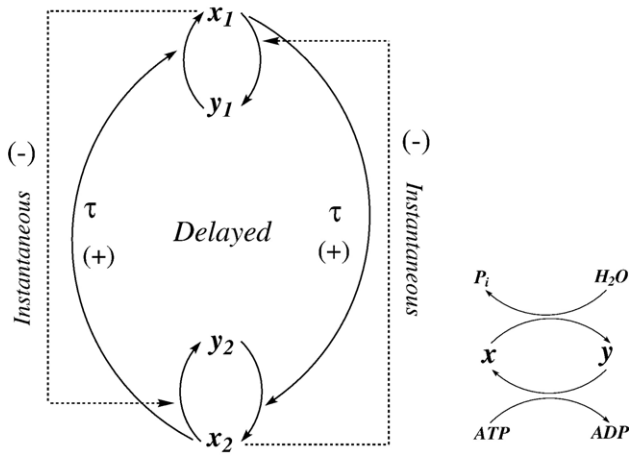

Fig. 2. Schematic representation of delayed network of phosphorylation–dephosphorylation cycles with delay in the positive regulatory steps. The co-factors involved in one phosphorylation–dephosphorylation cycle are given on the right of the schematic model. The cycles II and IV in Fig. 1 are now replaced with the delayed positive regulation (solid lines), where τ is the positive regulatory delay. The negative regulation is instantaneous (dashed lines).

maintained as equal. We have chosen this parameter set because it facilitates our mathematical analysis of the system. However, one can expect complex behavior for varying parameters. The variables x_1 and x_2 in our DDE model correspond to the X_1 and X_3 of the ODE model. From here on, we represent the variables of the DDE model in lower case. Similar to the ODE model, the concentrations of the PD pairs are scaled to unity ($x_i+y_i=1$). Here τ is the positive regulatory delay.

2.1. Simulation and results

The equations were solved using 'dde23.m' [20], a delay differential equation solver in Matlab. The two variable DDE model for $\tau=3$, qualitatively reproduced the behavior of the four variable ODE model. The delay value chosen is 3 because both the DDE and ODE model shows similar frequency and amplitudes. However, we describe the behavior of the DDE system for other delays in the further sections. The time series and the phase space diagrams of ODE model are shown in Fig. 3a and b and that of the DDE model for $\tau=3$ are shown in Fig. 3c and d. The time series of both the DDE and ODE models are similar after an initial transient. The 2D phase space of the variables x_1 and x_2 of the DDE model also resembles the phase space of X_1 and X_3 of the ODE model.

A system with delayed variables is infinite dimensional and as a consequence a two dimensional phase plane could be an over simplification. The phase plane of the DDE model seems to lack uniqueness with a crossing of trajectories. To illustrate the uniqueness of the solution, the time series of x_1 was reconstructed and embedded in a 3D phase space. It shows no crossing of trajectories, and hence it illustrates that the solution is unique. The attractor was reconstructed from the time series [21,22] by fixing the lag time [23]. Fig. 3e and f show the reconstructed phase space of the DDE model and 3D phase space of the ODE model.

2.2. Comparison of DDE and ODE models

DDE model exhibits other observed properties of the ODE model like effect of inhibitor, stability diagrams and parameter phase planes for a wide range of delays. Results are not shown because they are qualitatively similar to the ODE parameter phase planes and stability diagrams. Here we illustrate one situation where there are unsymmetrical positive and negative regulatory delays, which is similar to the case of unsymmetrical parameters in the ODE model.

2.2.1. Presence of unsymmetrical positive regulatory delays

In the above simulations, the positive regulatory delay exerted by cycle I and cycle II was maintained equal, thus representing a symmetrical condition. We have investigated the behavior of the system with two different positive regulatory delays, i.e., the delay for cycle I to activate cycle II being different from the delay for cycle II to activate cycle I. The resulting behavior is shown in Fig. 4b. We see a mild shift in the oscillatory profile of the variables when compared to the symmetrical case. It is interesting to note that this behavior is qualitatively similar to a situation in the ODE model with unsymmetrical V_{Mi} values, i.e., ($V_{M1}\neq V_{M2}\neq V_{M3}\neq V_{M4}$). Thus the case of unsymmetrical maximum rates (V_M) in the network can be qualitatively represented by larger or smaller delay in the sequential activation process of the DDE model. Fig. 4a is the simulation of ODE model given for comparison [19, Fig. 7a].

Table 1
Equations describing reduced phosphorylation–dephosphorylation network with delay in positive regulation

$$\frac{dx_1}{dt} = V_{M1}\left[1+\alpha_1\frac{x_2(t-\tau)}{K_{a1}+x_2(t-\tau)}\right]\frac{(1-x_1)}{K_1+(1-x_1)} - V'_{M1}\left[1+\beta_1\frac{x_2}{K_{b1}+x_2}\right]\frac{x_1}{K'_1+x_1} \quad (2)$$

$$\frac{dx_2}{dt} = V_{M2}\left[1+\alpha_2\frac{x_1(t-\tau)}{K_{a2}+x_1(t-\tau)}\right]\frac{(1-x_2)}{K_2+(1-x_2)} - V'_{M2}\left[1+\beta_2\frac{x_1}{K_{b2}+x_1}\right]\frac{x_2}{K'_2+x_2} \quad (3)$$

Parameter (i=1,2)	Description	values
V_{Mi}	Maximum rate of the phosphorylation reaction	1
V'_{Mi}	Maximum rate of the dephosphorylation reaction	1
K_i	Michaelis–Menten constant for phosphorylation process	0.01
K'_i	Michaelis–Menten constant for dephosphorylation process	0.01
K_{ai}	Michaelis–Menten constant for positive regulation	0.5
K_{bi}	Michaelis–Menten constant for negative regulation	0.5
α_i	Strength of positive regulation	1
β_i	Strength of negative regulation	1
τ	Positive regulatory delay	3

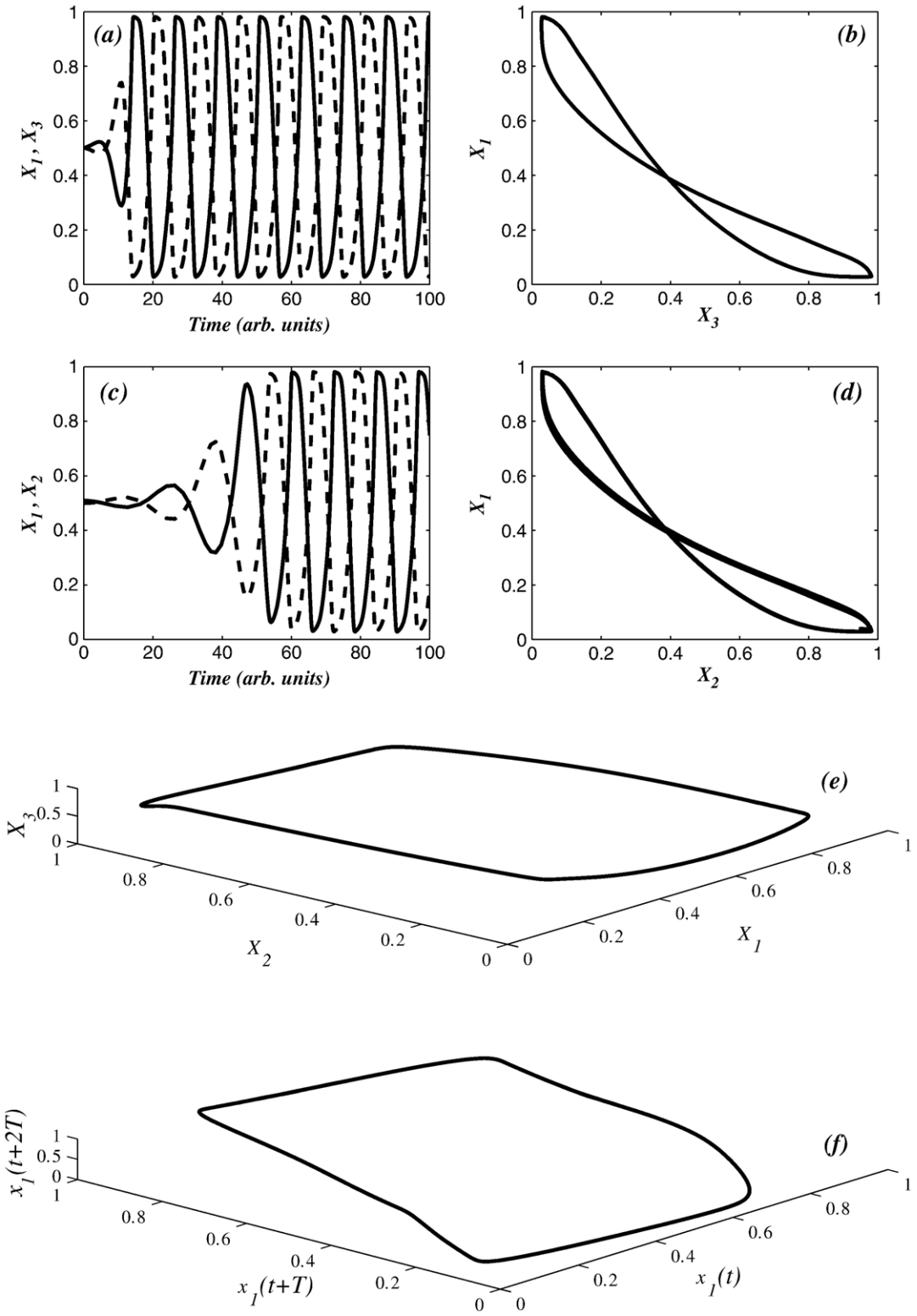

Fig. 3. Comparison of time series and phase space of the ODE and the DDE model. (a) – (b) Represent time series and phase portrait of ODE model respectively, (c) – (d) Represent time series and phase portrait of DDE model respectively for $\tau=3$. X_1, x_1 are denoted by solid lines and X_3, x_2 are denoted by dashed lines. The 2D phase portrait of both ODE and DDE models are identical. (e) Shows the 3D phase portrait of the ODE model (f) Shows the reconstructed phase portrait of DDE model.

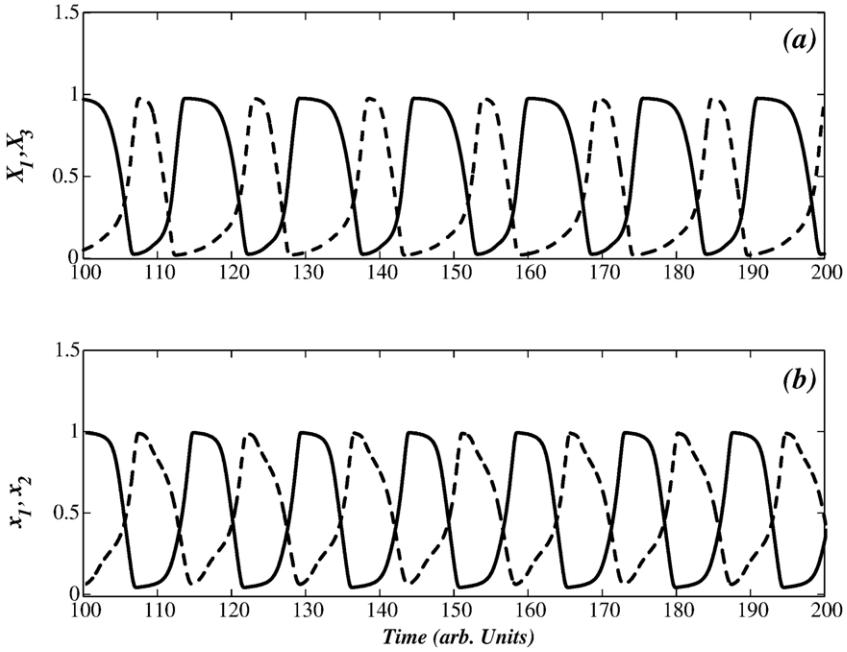

Fig. 4. Presence of unsymmetrical positive regulatory delays. (a) Time course of X_1 and X_3 of ODE model with parameters $V_{M1}=0.99$, $V_{M2}=0.9$, $V_{M3}=1.1$, $V_{M4}=1.1$ (b) Time course of x_1 and x_2 of DDE model with unsymmetrical positive regulatory delays ($\tau=5, 2.5$). X_1, x_1 are denoted by solid lines and X_3, x_2 are denoted by dashed lines. Note that (a) and (b) are similar.

Various stability diagrams and parameter diagrams were constructed for the DDE model using DDE-BIFTOOL [24]. They were qualitatively similar to the ODE model for a wide range of delays (results not shown).

2.3. Two parameter diagram of delay and ratio of maximum rates

Different delays can result in different dynamical behavior of the system such as a stable steady state or a limit cycle solution. To identify various dynamical features caused by delay, we investigate the two parameter diagram of delay and the ratio of maximum rates which is defined as $r=V_{Mi}/V'_{Mi}$. The two parameter diagram of delay τ and r is shown in Fig. 5. Notice that the diagram can be divided into four regions with three dynamical behaviors: stable steady state, stable limit cycle and hard excitation. Hard excitation, also called a sub-critical Hopf bifurcation, is the co-existence of a stable steady state and a stable limit cycle along with an unstable limit cycle.

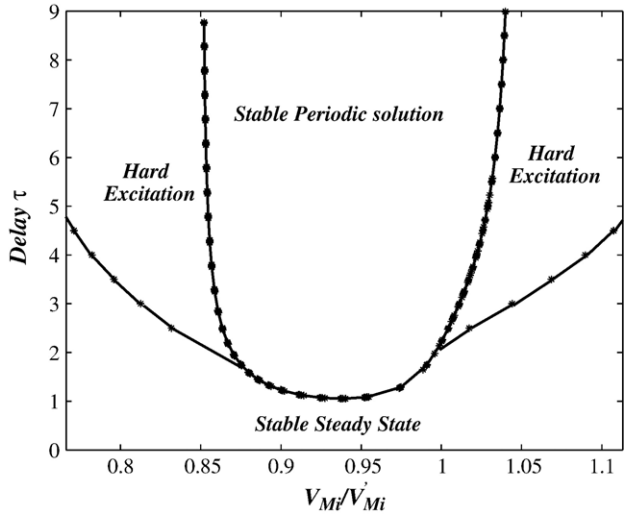

Fig. 5. Two parameter diagram of r and τ. The diagram shows three types of regions: stable steady state, stable limit cycle and hard excitation regimes.

In the model, limit cycle oscillations do not occur for lower values of delay because (phosphorylated product) cycle I activates the phosphorylation step of cycle III instantaneously. The (phosphorylated product) cycle III in turn instantaneously exerts a negative feedback on cycle I and hence results in no oscillation. This situation exists until a threshold delay is introduced in the activation step which is reflected subsequently in the negative regulation, resulting in oscillations. We have seen that a network of four cycles can be reduced to two with delay in positive regulation. This situation can be extended to networks consisting of N cycles, which can be reduced into an $N/2$ cycle network using positive delayed regulation.

2.4. Quantitative comparison of the ODE and DDE models

Quantitative comparison of the ODE and DDE models would be valuable information when reducing an ODE into a DDE model. However, in this case, the amplitude of the oscillations would be quantitatively the same for both the ODE and the DDE systems, due to the normalization of the

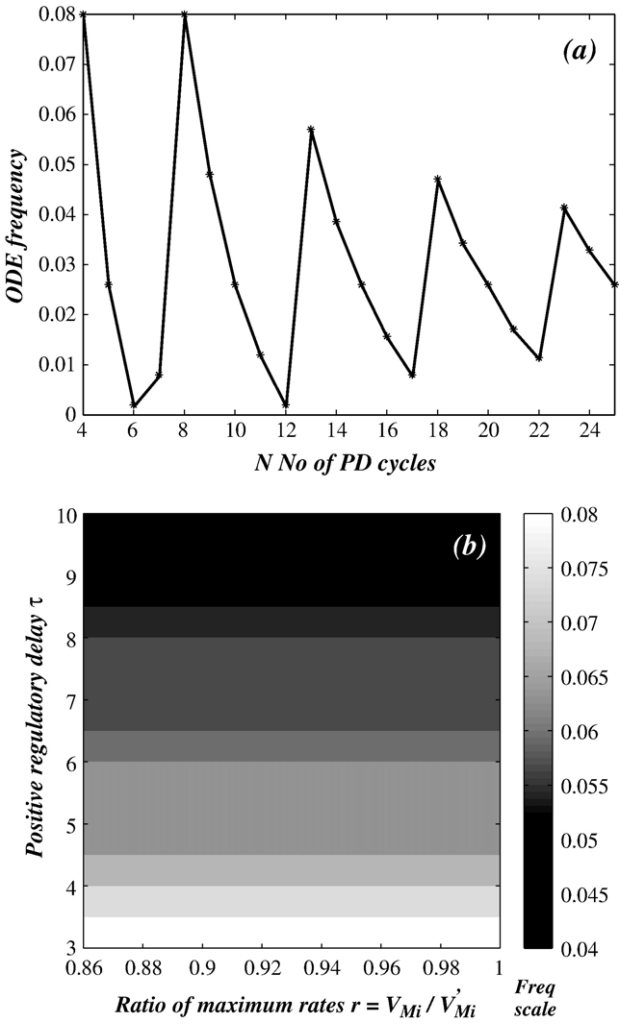

Fig. 6. (a) Variation of frequency of the ODE model with N (No. of PD cycles) (b) Variation of frequency of the DDE model in the $\tau - r$ space. Frequency scale varies from high to low as the color moves from light to dark.

concentrations. However, the frequency of the oscillations will vary. The mathematics involved in deriving an expression of frequency in terms of the parameters is too complex to be useful, due to the intricate nature of the system (see Section 3.3). In order to bring in a quantitative comparison between the ODE and the DDE frequencies we computed the following numerically.

- Variation of frequency of the ODE models as a function of N as given in Fig. 6a
- Variation of frequency in the $\tau - r$ space which is given in Fig. 6b.

If we reduce an ODE system into a DDE under symmetrical conditions, we can compare Fig. 6a and b and choose the appropriate delay values to achieve the same amplitude and frequency. For example, when $N=4$, the ODE and the DDE frequency quantitatively coincide at $\tau=3$. However, further straightforward comparison would be difficult.

3. Reduced model with delayed positive and negative regulations

We can reduce a network of N PD cycles into a delayed network of $N/2$, provided N is even. Is it possible to model an N cycle network with just two PD cycles instead of $N/2$ with delayed interactions? We note from Fig. 5 that within a range of $r(=0.87-0.99)$, limit cycle oscillations with large time periods exist even for very high delay values. So it is possible to achieve any time period with delay in the positive regulatory step. However, we found that the phase relationship between the two variables of the DDE model (Table 1) is always π. In contrast, in a N variable ODE model, the phase relationship between the variables varies. Therefore, a network with delays in both positive and negative regulatory steps could produce new phase relationships, enabling us then to model N cycle network with two PD cycles. Thus this section discusses the combined effect of introducing delay in both positive and negative regulatory steps in the DDE model. We call this model a Delayed Positive and Negative Regulatory model (DPNR).

The DPNR model is schematically represented in Fig. 7. The positive regulatory delay is τ_1 and negative regulatory delay is τ_2. In a network of N cycles where N is even, we choose the first cycle and $(N/2)+1$th cycle as the two variables in the DDE model. The rest of the intermediate cycles are represented as delayed positive and negative regulations. Therefore, for an N cycle network, the two variables of the DDE model are named as x_1 and $x_{N/2+1}$ to represent X_1 and $X_{N/2+1}$ of the ODE model. For example, the DDE variables are x_1 and x_3 for $N=4$. In Table 2 we show Eqs. (4) and (5) governing the DPNR model for a network of N cycles (provided N and $N/2$ are even). The parameters are described in Table 1.

3.1. Simulation and results

Two oscillatory regimes are observed for two different cases namely, $\tau_1 > \tau_2$ and $\tau_2 > \tau_1$. For a fixed value of τ_1, when

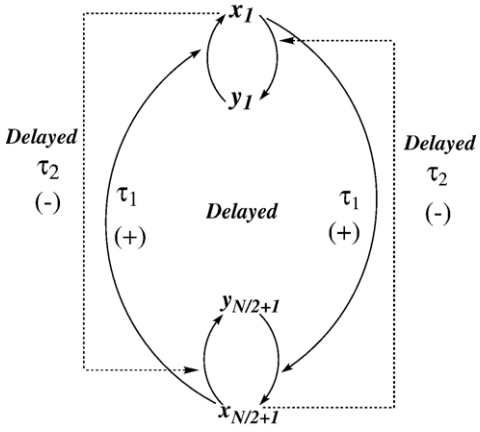

Fig. 7. Schematic representation of delayed network of phosphorylation–dephosphorylation cycles with delay in the positive (τ_1) and negative (τ_2) regulatory steps. The two delays now replace more than one cycle in between the first cycle and the $(N/2)+1$th cycle.

Table 2
Equations governing DPNR model

$$\frac{dx_1}{dt} = V_{M1}\left[1+\alpha_1\frac{x_{N/2+1}(t-\tau_1)}{K_{a1}+x_{N/2+1}(t-\tau_1)}\right]\frac{(1-x_1)}{K_1+(1-x_1)} - V'_{M1}\left[1+\beta_1\frac{x_{N/2+1}(t-\tau_2)}{K_{b1}+x_{N/2+1}(t-\tau_2)}\right]\frac{x_1}{K'_1+x_1} \quad (4)$$

$$\frac{dx_{N/2+1}}{dt} = V_{M2}\left[1+\alpha_2\frac{x_1(t-\tau_1)}{K_{a2}+x_1(t-\tau_1)}\right]\frac{(1-x_{N/2+1})}{K_2+(1-x_{N/2+1})} - V'_{M2}\left[1+\beta_2\frac{x_1(t-\tau_2)}{K_{b2}+x_1(t-\tau_2)}\right]\frac{x_{N/2+1}}{K'_2+x_{N/2+1}} \quad (5)$$

The nomenclature x_1 and $x_{N/2+1}$ represents the corresponding cycles in the network.

$\tau_2 \ll \tau_1$, we find antiphase oscillations. As we increase the value of τ_2, the antiphase oscillations disappear and the two variables coincide with each other so that the phase difference is zero. We call this situation inphase or zerophase oscillations.

No oscillations occur for $\tau_1=\tau_2$. We do not observe oscillations for other values of τ_1 and τ_2 close to $\tau_1=\tau_2$. We analytically show the existence of the stability region above and below $\tau_1=\tau_2$ in Section 3.3, which is consistent with numerical simulations. As we increase τ_2 further such that $\tau_2>\tau_1$, antiphase oscillations reappear. Following the antiphase oscillations, the zerophase oscillations reappear for very high values of τ_2.

The trend observed for a fixed τ_1 value as a function of τ_2 is schematically represented in Fig. 8. Note that the antiphase and zerophase oscillations alternate. It is very interesting to note that the system can exhibit only two phase relationships namely the antiphase and zerophase, irrespective of the delays. The limit cycles of both the antiphase oscillations are close to being mirror images of each other as in Fig. 9. The two limit cycles (red-dotted and blue-solid) denote the cases, namely $\tau_1>\tau_2$ and $\tau_1<\tau_2$.

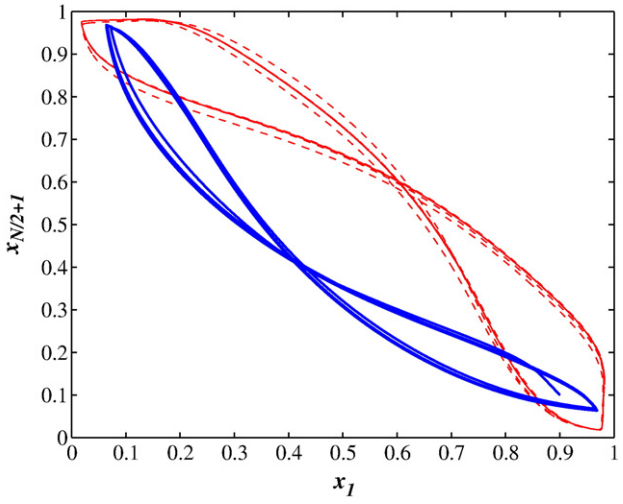

Fig. 9. Phase portrait of the limit cycles of the DPNR model. The red dotted curves show the phase portrait for $\tau_1=3$ and $\tau_2=6$. The solid blue curves show the phase portrait for $\tau_1=3$ and $\tau_2=0.5$. We see that the limit cycles are in fact close to being mirror images of each other, representing the symmetrical nature of the system. (For interpretation of the references to colour in this figure legend, the reader is referred to the web version of this article.)

We explored the properties such as the effect of the inhibitor, the presence of positive regulation only ($\beta=0$), presence of negative regulation only ($\alpha=0$) and two parameter diagrams ($K-r$, $\alpha-\beta$ and $K-K_a$) in both ODE and the DPNR models. We do not find any qualitative difference between the models (results not shown).

3.2. The τ_1-r, τ_2-r and $\tau_1-\tau_2$ diagrams

The significant two-parameter diagrams are τ_1-r, τ_2-r and $\tau_1-\tau_2$. Since we observe two distinct oscillatory regimes we expect the same behavior in the parameter diagrams. The $\tau_1-\tau_2$

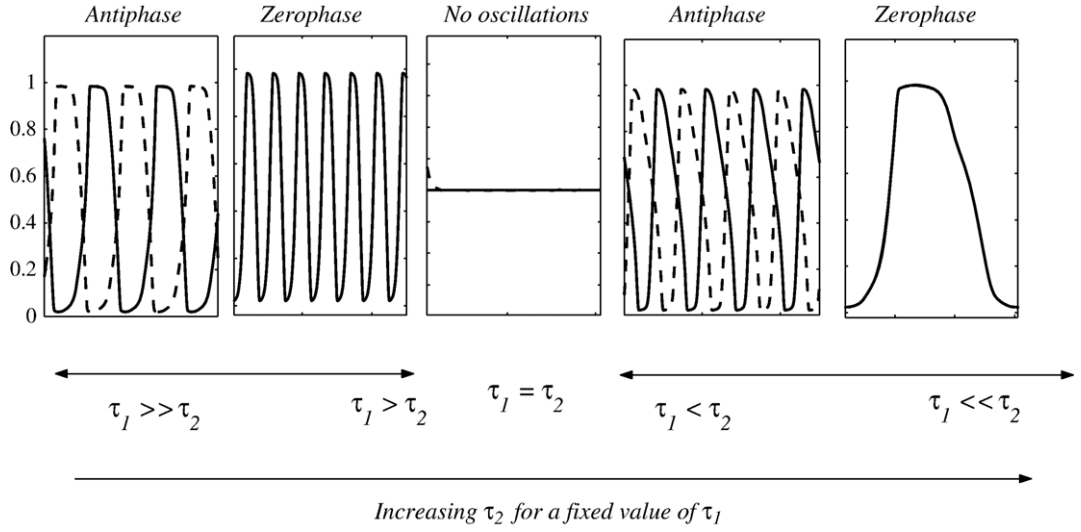

Fig. 8. Schematic representation of the different behaviors as a function of τ_2. We observe a transition from antiphase to zerophase followed by a stable steady state. For $\tau_1<\tau_2$ the antiphase oscillations reappear followed by a transition into zerophase oscillations.

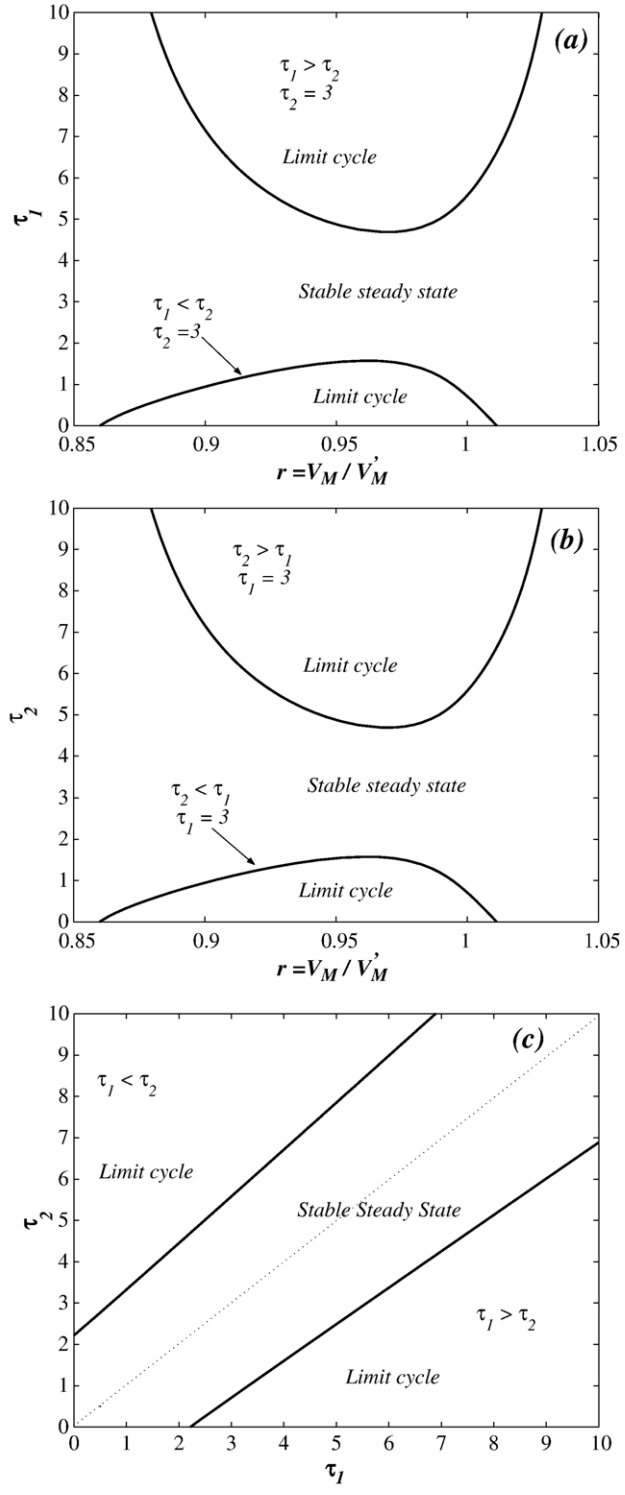

Fig. 10. Parameter diagrams for DPNR model. (a) Shows the τ_1-r diagram for a constant $\tau_2=3$. (b) Shows the τ_2-r diagram for a constant $\tau_1=3$. (c) Represents $\tau_1-\tau_2$ diagram for $r=1$. In (c) we observe a region above and below $\tau_1=\tau_2$ for which the system is stable.

diagram is given in Fig. 10c, which distinctly shows two oscillatory regimes for the two cases, namely $\tau_1>\tau_2$ and $\tau_2>\tau_1$. We do not observe oscillations for $\tau_2=\tau_1$ (indicated by dotted line in Fig. 10c) and for a small region above and below the $\tau_2=\tau_1$ line. We find a similar trend for other parameter diagrams, namely τ_1-r for constant τ_2 (Fig. 10a) and τ_2-r for constant τ_1 (Fig. 10b).

3.3. Linear stability analysis for two delay model

The rate equations in Table 1 may be rewritten in the following form for convenience

$$\frac{dx_1}{dt}=f_1+f_2 \tag{6}$$

$$\frac{dx_2}{dt}=g_1+g_2, \tag{7}$$

where

$$f_1=V_{M1}\left[1+\alpha_1\frac{x_2(t-\tau_1)}{K_{a1}+x_2(t-\tau_1)}\right]\frac{(1-x_1)}{K_1+(1-x_1)} \tag{8}$$

$$f_2=-V'_{M1}\left[1+\beta_1\frac{x_2(t-\tau_2)}{K_{b1}+x_2(t-\tau_2)}\right]\frac{x_1}{K'_1+x_1} \tag{9}$$

$$g_1=V_{M2}\left[1+\alpha_2\frac{x_1(t-\tau_1)}{K_{a2}+x_1(t-\tau_1)}\right]\frac{(1-x_2)}{K_2+(1-x_2)} \tag{10}$$

$$g_2=-V'_{M2}\left[1+\beta_2\frac{x_1(t-\tau_2)}{K_{b2}+x_1(t-\tau_2)}\right]\frac{x_2}{K'_2+x_2}. \tag{11}$$

The Jacobian J is formulated by assuming the perturbation to be proportional to $e^{\lambda t}$ and thus, making $x(t-\tau)=x(t)e^{-\lambda\tau}$ and differentiating, we get

$$J=\begin{pmatrix}\dfrac{\partial f_1}{\partial x_1}+\dfrac{\partial f_2}{\partial x_1} & \dfrac{\partial f_1}{\partial x_2}e^{-\lambda\tau_1}+\dfrac{\partial f_2}{\partial x_2}e^{-\lambda\tau_2}\\ \dfrac{\partial g_1}{\partial x_1}e^{-\lambda\tau_1}+\dfrac{\partial g_2}{\partial x_1}e^{-\lambda\tau_2} & \dfrac{\partial g_1}{\partial x_2}+\dfrac{\partial g_2}{\partial x_2}\end{pmatrix}. \tag{12}$$

The above Jacobian is evaluated at the steady state and the stability is found by solving the characteristic equation. The steady state is dependent on all the parameters. We define a symmetric condition as follows: $V_{Mi}=V'_{Mi}=1$, $\alpha_i=\beta_i=1$, $K_i=K'_i=0.01$ and $K_{ai}=K_{bi}=0.5$, the steady states are $x^*=0.5, y^*=0.5$. The resulting characteristic equation is of the form

$$\lambda^2+2a\lambda+2b^2e^{-\lambda(\tau_1+\tau_2)}-b^2e^{-2\lambda\tau_1}-b^2e^{-2\lambda\tau_2}+a^2=0. \tag{13}$$

In this expression,

$$a=-\left(\frac{\partial f_1}{\partial x_1}+\frac{\partial f_2}{\partial x_1}\right)=-\left(\frac{\partial g_1}{\partial x_2}+\frac{\partial g_2}{\partial x_2}\right),$$
$$b=\frac{\partial f_1}{\partial x_2}=-\frac{\partial f_2}{\partial x_2}=\frac{\partial g_1}{\partial x_1}=-\frac{\partial g_2}{\partial x_1}, \tag{14}$$

are evaluated at the steady state $x^*=0.5$, $y^*=0.5$. The above characteristic equation is transcendental in nature and can be solved numerically to obtain the eigenvalues. The stability properties may be obtained for this symmetrical condition by examining the properties of the above expression at Hopf bifurcation, namely when $\lambda=i\omega$ [25].

Table 3
Phase difference between two adjacent variables of ODE model for large N values

N — no. of cycles	ϕ_{ODE} — phase difference between two adjacent variables
4–7	$\frac{2\pi}{N}$
8–12	$\frac{4\pi}{N}$
13–17	$\frac{6\pi}{N}$
18–22	$\frac{8\pi}{N}$
23–27	$\frac{10\pi}{N}$

Note that the span of the phase increases by 2π for every five cycles.

To examine the nature of the system when the roots are purely imaginary, we substitute $\lambda = i\omega$ in the characteristic equation. After some steps of expanding $e^{-i\omega\tau}$ into sin and cos terms and rearranging, we get the real and imaginary parts separated as

$$\cos(\omega\tau_1 + \omega\tau_2)[\cos(\omega\tau_1 - \omega\tau_2) - 1] = \frac{a^2 - \omega^2}{2b^2} \tag{15}$$

$$\sin(\omega\tau_1 + \omega\tau_2)[\cos(\omega\tau_1 - \omega\tau_2) - 1] = \frac{-a\omega}{b^2}. \tag{16}$$

Squaring and adding we obtain

$$[\cos(\omega\Delta\tau) - 1]^2 = \left[\frac{a^2 + \omega^2}{2b^2}\right]^2, \tag{17}$$

where $\Delta\tau = \tau_1 - \tau_2$. The roots of Eq. (17) are

$$\cos(\omega\Delta\tau) - 1 = \pm\Theta, \tag{18}$$

with $\Theta = (a^2 + \omega^2)/2b^2$. When $\tau_1 = \tau_2$, $\Delta\tau = 0$ and eventually $a^2 + \omega^2 = 0$ implying that the roots are imaginary and that there cannot be oscillations for this condition. This is also observed in the numerical simulation of the $\tau_1 - \tau_2$ parameter space.

We see that Eq. (18) has four roots which can be called ω_{1+}, ω_{2+} and ω_{1-}, ω_{2-}. It is possible to examine Eq. (18) for positive ω. However, even with the present condition it is interesting to note that there is a stability switch of the steady state from unstable to stable and back to unstable as the $\Delta\tau$ moves from a negative value to a positive value.

Let $\Delta\tau\omega = \theta$. Now $\cos\theta = 1 \pm \Theta$. For $\cos\theta > 0$, θ should lie in the first or fourth quadrant, i.e., $-\pi/2 < \theta < \pi/2$. Therefore, if there is a critical $\Delta\tau$, above which there is a stability change from stable to unstable, the same condition holds good for $-\Delta\tau$ implying that there is a region in the $\tau_1 - \tau_2$ diagram above and below $\Delta\tau = 0$ such that $-\Delta\tau_c < \Delta\tau < \Delta\tau_c$ where the system is stable between this range [26, Chapter 6]. This is in fact observed in the numerical bifurcation diagram. From Eq. (18) we obtain

$$\Delta\tau = \frac{1}{\omega}\cos^{-1}[1 \pm \Theta] = \frac{\theta + 2n\pi}{\omega}. \tag{19}$$

With the above equation, according to Cooke and Grossman [25], a finite number of stability switches are present before there is instability for all $\Delta\tau$ greater than $\Delta\tau_c$. However, after further analysis we find that it is not possible to solve analytically. Hence we have to resort to numerical methods to determine the behavior of the system.

3.4. Comparison of N cycle ODE model with DPNR model

To compare the DDE and ODE models, we need to understand the behavior of the ODE model for large N. The properties of the ODE model with large N are briefly discussed in [19]. We conduct further investigations that reveal some interesting properties of the ODE model. Comparison between the ODE and DDE models can be made in terms of the phase difference between the variables in their time course. We also found that the phase difference ϕ_{ODE} between any two adjacent variables of ODE model is dependent on the number of cycles N

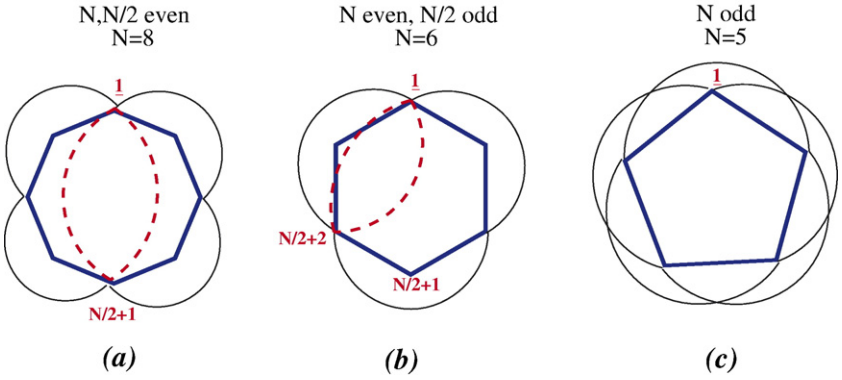

Fig. 11. Schematic diagram of N cycle network showing the negative regulations alone. The edges of the thick solid polygons represent a PD cycle. The thin solid black curves indicate the negative regulatory interactions on alternate cycles for (a) $N=8$ (b) $N=6$ and (c) $N=5$ of the ODE model. The red dotted lines indicate the possible delayed negative regulatory interaction of the DDE model. (For interpretation of the references to colour in this figure legend, the reader is referred to the web version of this article.)

in the network. Table 3 gives the phase difference between any two adjacent variables in the ODE model for large N values, whereas the phase difference between the two variables of the DDE model can only be 0 or π. We now split the ODE system into 3 cases, namely (a) N and $N/2$ even (b) N even and $N/2$ odd and (c) finally N odd and discuss the similarities between the ODE and DDE model in detail.

3.4.1. N and N/2 even

In the ODE model, the phase difference (Φ) between first and $(N/2)+1$th variable is either 0 (zerophase) or π (antiphase). For example $\Phi=\pi$ for $N=4$ and $\Phi=0$ for $N=8$, and so on. This is indeed the phase relationships exhibited by the DDE model. Thus, by appropriately choosing τ_1 and τ_2, a N-variable ODE system can be represented by a two-variable DDE system for all N and $N/2$ even.

3.4.2. N even and N/2 odd

In the previous case, the first cycle exerts a delayed negative feedback on the $(N/2)+1$th cycle (see Fig. 11a), whereas in this case the first cycle exerts the negative feedback on the $(N/2)+2$th cycle of ODE model (see Fig. 11b). Therefore, if we choose to represent this case with a two variable DDE system, then the two variables should actually correspond to first and $(N/2)+2$th cycle of the ODE system.

But the phase difference Φ between the first and $(N/2)+2$th variable of the ODE system is not always 0 or π, while the phase difference in DDE model is always either 0 or π. Hence, a two variable DDE is not enough to represent the network of N cycles where N is even and $N/2$ is odd. However, this case can be still represented by $N/2$ DDEs to qualitatively represent the dynamics.

3.4.3. N odd

In this case, as in Fig. 11c, the negative feedback is interlocked such that it is difficult to choose the two variables to be represented by the DPNR model. Also the phase difference varies according to the value of N. Therefore, it is not possible in a two variable DPNR model to represent networks with large N, where N is an odd number. Further investigation is required to determine the minimum number of delay variables needed for this case. A summary of the above findings is tabulated in Table 4. According to our results, we can represent N cycle network with just two variables of a DDE model when N and $N/2$ are even. When N is even and $N/2$ is odd, then we can represent the situation using $N/2$ variables in a DDE model. If N is odd, then representation with a delay model may be difficult or often involve more interlocked variables. Thus we outline an idea about how many cycles can be replaced using DDE model.

Table 4
Reference table for representing N variable ODE model with DDE model with fewer number of variables

N	$N/2$	N_d
Even	Even	2
Even	Odd	$N/2$
Odd	–	>2

N_d — no. of delayed variables required to reproduce the phase difference of ODE model.

4. Discussion

Many biochemical pathways operate on networks consisting of several phosphorylation–dephosphorylation cascades. There is a relay of signal propagation by a series of PD cycles coupled with positive and negative regulations. The system we studied here is a general model representing such a relay linked in a cyclic manner.

DDEs can be used to describe a system with reduced number of variables. In this paper we carried out a systematic comparison of DDE and ODE models governing a cyclic PD network, which is, as far as we know, the first study of this kind. Our objective was to provide explanations for three questions:

(1) Is it possible to model PD cascades with delayed regulations and a minimum number of variables?
(2) What are the new dynamical features of the DDE model?
(3) What are the minimum number of variables in the DDE model required to model the PD network?

We addressed the first question by introducing delays in positive regulatory step of the PD network. We illustrated that the DDE model exhibits similar dynamics as that of the ODE model (Section 2.2). We extended our analysis by introducing the Delay in Positive and Negative Regulation model (DPNR model) to represent networks with large number of PD cycles.

Our analysis of the DPNR model revealed unique properties in the DDE model such as the two oscillatory regimes for two different conditions namely $\tau_1>\tau_2$ and $\tau_1<\tau_2$, and the absence of oscillations for $\tau_1=\tau_2$. Another interesting result of the DPNR model is that we observed only antiphase and zerophase relationships between the two variables.

To address the third question, as a first step, we conducted further analysis on the parent network and the ODE model. Our study brought out the following important properties:

- We observed that the span of the total phase for ODE model increases by a factor of 2π for the addition of every five cycles in the network. This aided in the identification of those variables with zero and antiphase relationships in the ODE model (see Table 3).
- We constructed the topology of the N cycle PD network (Fig. 11) connected through negative regulations, in order to identify variables connected through negative feedback.

As a second step, we used the above properties to compare the ODE and the DPNR models with respect to their phase relationships. We then systematically summarized the minimum number of delay variables required to represent N cycle network in Table 4 that can serve as a reference table.

Delay has been used for various purposes in modeling biochemical networks: (1) To account for genuine time lags such as incubation time or aging time that occurs in biological systems [10] (2) To describe the core structure of the dynamics

with few variables and parameters [13]. However, when we use delays to model large networks with fewer variables, it is to be noted that those cycles or steps that are replaced with delay are still biologically very important. The importance of the presence of futile cycles in terms of energy balance has been discussed by Qian and Beard [27]. He has theoretically proved that futile cycles serve as biochemical regulators by increasing the robustness and sensitivity. In a specific case of two cascading PD cycles similar to our network, Qian showed that the ATP hydrolysis cycle powers the biochemical transition between the phosohorylated and dephosphorylated forms [28].

Our approach to model large scale networks with DDEs does not underestimate the importance of redundant cycles. The use of delay for replacing redundant cycles aids in the conceptual understanding of large scale systems. Further, it is not always possible to experimentally measure each and every step in a cascade, wherein the delay becomes useful in understanding the system with minimal information.

It is believed that redundant cycles help in fine-tuning the energetics of the system, as a consequence they do not seem to be an important part of the core dynamical structure. In other words, these cycles do not alter the dynamic uniqueness of a system. So while modeling these networks with bits and pieces of information from the experiments, it would be valuable to obtain a simpler model that would enhance the overall understanding.

The applicability of our results has been tested in a PD cascade that is explicitly present in the activation step of APC (anaphase promoting complex) by MPF (maturation promoting factor) in cell cycle dynamics. The idea of replacing cascading PD cycles by delayed regulations has been implemented in a cell cycle model by Srividhya and Gopinathan [29]. The model discusses the possible role of delay as a spindle checkpoint during the cell cycle. The delay brings in an interesting feature, namely the extension of G1 phase, which has been observed in experiments.

A limitation of the DPNR model is that it describes the similarities between the DDE and the ODE models (in terms of phase differences between the variables) qualitatively. A quantitative comparison in terms of frequency and amplitude could throw more light on practical application of our results. One should implement the above findings in models with caution since biochemical pathways may have several inter-linked regulatory loops. It is to be noted that this study is strictly valid to a particular class of PD networks.

Large scale modeling of complex systems to understand their dynamics is actively in progress. Simplifying the systems with delays could prevent spending time on redundant mechanisms and focus on the key regulators of the dynamics. Thus the DPNR model described in this paper shows that complex cascading networks consisting of PD cycles can be simplified in a systematic way using delayed interactions.

Acknowledgements

We are grateful to the two anonymous referees for their helpful comments. We thank Dr. Ramon Grima (Indiana University) for a critical review, Dr. K. Sriram, Epigenomics, (Genopole, France) for his valuable suggestions. We also thank Dr. Keon Engelborghs (K.U.Leuven, Belgium), for providing the DDE-BIFTOOL software. This work was supported by the Council of Scientific and Industrial Research (CSIR—India) and National Science Foundation (NSF) Grant IIS-0513701. Any opinions, findings, and conclusions or recommendations expressed in this paper are those of the authors and do not necessarily reflect the views of the NSF and CSIR.

References

[1] S. Chu, T.J. Ferroa, Sp1: regulation of gene expression by phosphorylation, Gene 348 (2005) 1–11.
[2] L. Kornberg, H.S. Earp, J.T. Parsons, M. Schaller, R.L. Juliano, Cell adhesion or integrin clustering increases phosphorylation of a focal adhesion-associated tyrosine kinase, J. Biol. Chem. 267 (1992) 23439–23442.
[3] M.G. Lee, C.J. Norbury, N.K. Spurr, P. Nurse, Regulated expression and phosphorylation of a possible mammalian cell-cycle control protein, Nature 333 (1988) 676–679.
[4] G.L. Razidlo, R.L. Kortum, J.L. Haferbier, R.E. Lewis, Phosphorylation regulates ksr1 stability, erk activation, and cell proliferation, J. Biol. Chem. 279 (2004) 47808–47814.
[5] M. Marchisio, E. Santavenere, M. Paludi, A.R. Gaspari, P. Lanuti, A. Bascelli, E. Ercolino, A.D. Baldassarre, S. Miscia, Erythroid cell differentiation is characterized by nuclear matrix localization and phosphorylation of protein kinases c (pkc) alpha, delta, and zeta, J. Cell. Physiol. 205 (2005) 32–36.
[6] A.W. Murray, M.W. Kirschner, Dominoes and clocks: the union of two views of the cell cycle, Science 246 (1989) 614–621.
[7] A. De Gaetano, O. Arino, Probabilistic determination of stability for delay-differential model of the glucose-insulin dynamical system, J. Biol. Syst. 7 (1999) 131–144.
[8] S. Marino, S. Ganguli, I.M.P. Joseph, D. Kirschner, The importance of an inter-compartmental delay in a model for human gastric acid secretion, Bull. Math. Biol. 65 (2003) 963–990.
[9] J. Bèlair, M.C. Mackey, J.M. Mahaffy, Age-structured and two-delay models for erythropoiesis, Math. Biosci. 128 (1995) 317–346.
[10] B. Bernard, J. Bèlair, M.C. Mackey, Oscillations in cyclical neutropenia: new evidence based on mathematical modeling, J. Theor. Biol. 223 (2003) 283–298.
[11] N. Yildirim, M.C. Mackey, Feedback regulation in the lactose operon: a mathematical modeling study and comparison with experimental data, Biophys. J. 84 (2003) 2841–2851.
[12] N.A.M. Monk, Oscillatory expression of Hes1, p53, and NF-kappaB driven by transcriptional time delays, Curr. Biol. 13 (2003) 1409–1413.
[13] T.J. Schepper, D. Klinkenberg, C. Pennartz, J.C. Pelt, A mathematical model for the intracellular circadian rhythm generator, J. Neurosci. 19 (1999) 40–47.
[14] P. Smolen, D.A. Baxter, J.H. Byrne, A reduced model clarifies the role of feedback loops and time delays in the Drosophila circadian oscillator, Biophys. J. 83 (2002) 2349–2359.
[15] K. Sriram, M.S. Gopinathan, A two variable delay model for the circadian rhythm of *Neurospora crassa*, J. Theor. Biol. 231 (2004) 23–38.
[16] I.R. Epstein, Delay effects and differential delay equations in chemical kinetics, Int. Rev. Phys. Chem. 11 (1992) 135–160.
[17] M.R. Roussel, The use of delay-differential equations in chemical kinetics, J. Phys. Chem. 100 (1996) 8323–8330.
[18] R. Hinch, S. Schnell, Mechanism equivalence in enzyme-substrate reactions: distributed differential delay in enzyme kinetics, J. Math. Chem. 35 (2004) 253–264.
[19] D. Gonze, A. Goldbeter, A model for a network of phosphorylation–dephosphorylation cycles displaying the dynamics of dominoes and clocks, J. Theor. Biol. 210 (2001) 167–186.
[20] L.F. Shampine, S. Thompson, Solving DDEs in MATLAB, Appl. Numer. Math. 37 (2001) 441–448.

[21] F. Takens, Detecting Strange Attractors in Turbulence, Springer, New York, 1981, 366–381.
[22] N.H. Packard, J.P. Grutchfield, J.D. Farmer, R.S. Shaw, Geometry from a time series, Phys. Rev. Lett. 45 (1980) 712–716.
[23] D.T. Kaplan, L. Glass, Understanding Non-linear Dynamics, Springer-Verlag, New York, 1995.
[24] K. Engelborghs, T. Luzyanina, D. Roose, Numerical bifurcation analysis of delay differential equations using DDE-BIFTOOL, ACM Trans. Math. Softw. 28 (2002) 1–21.
[25] K.L. Cooke, Z. Grossman, Discrete delay, distributed delay and stability switches, J. Math. Anal. Appl. 85 (1982) 592–627.
[26] N. McDonald, Biological Delay Systems: Linear Stability Theory, Cambridge University Press, Cambridge, UK, 1989.
[27] H. Qian, D.A. Beard, Metabolic futile cycles and their functions: a systems analysis of energy and control, IEE Proc. Syst. Biol. 153 (2006) 192–200.
[28] H. Qian, Open-system nonequilibrium steady state: statistical thermodynamics, fluctuations, and chemical oscillations, J. Phys. Chem. B 110 (2006) 15063–15074.
[29] J. Srividhya, M.S. Gopinathan, A simple time delay model for eukaryotic cell cycle, J. Theor. Biol. 214 (2006) 617–627.